

MHD stagnation point flow over an unsteady stretching surface



By

Noor Muhammad

Supervised by

Dr. Zaheer Abbas

Department of Mathematics and Statistics
Faculty of Basic and Applied Sciences
International Islamic University, Islamabad
Pakistan
2011

Accession No. TH-8653

MS

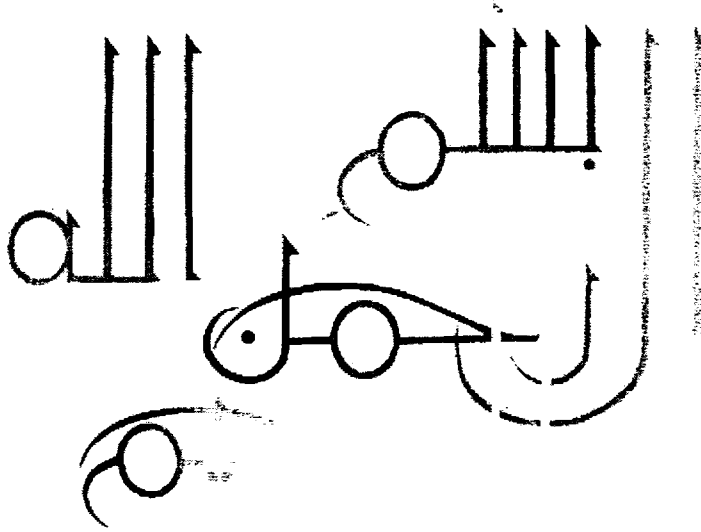
532.051

NOS

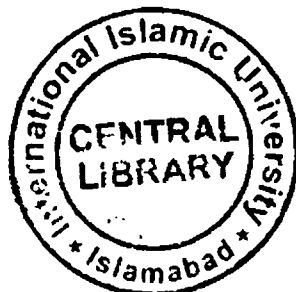
- 1- Flow; fluid mechanics
- 2- Fluid mechanics

DATA ENTERED

Amz 12/04/13



**In the name of Almighty ALLAH,
the most beneficent, the most merciful**



MHD stagnation point flow over an unsteady stretching surface



By

Noor Muhammad

Department of Mathematics and Statistics
Faculty of Basic and Applied Sciences
International Islamic University, Islamabad

Pakistan

2011

MHD stagnation point flow over an unsteady stretching surface

By

Noor Muhammad

A Dissertation Submitted in the Partial Fulfillment of the^s

Requirements for the Degree of

MASTER OF SCIENCE

In

Mathematics

Supervised by

Dr. Zaheer Abbas

Department of Mathematics and Statistics

Faculty of Basic and Applied Sciences

International Islamic University, Islamabad

Pakistan

2011

Certificate

MHD stagnation point flow over an unsteady stretching surface

By

Noor Muhammad

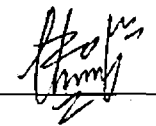
A Dissertation Submitted in the Partial Fulfillment of the Requirements for the Degree of

MASTER OF SCIENCE in Mathematics

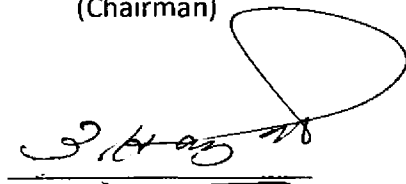
We accept this dissertation as confirming to the required standards.

1. 


Dr. Irshad Ahmad Arshad
(Chairman)

2. 

Dr. Zaheer Abbas
(Supervisor)

3. 

Prof. Dr. Tasawar Hayat
(External Examiner)

4. 

Dr. Nasir Ali
(Internal Examiner)

Dedicated to

My "Mother" and "Father"

Whose prayer has
Always been the reason of success and prosperity in my life

Acknowledgement

Primarily and foremost, I am thankful to **Almighty ALLAH** Who is the only creator and master of us, Who create us from a clot and taught us to write with pen, Who provided me the strength and ability to learn and to achieve another milestone to a destination. Countless drood -o- slam upon **Holy Prophet Hazrat MUHAMMAD (PBUH)** Who is forever a torch of gaudiness, a source of knowledge and blessing for entire creation. His teaching shows us a way to live with dignity, stand with honor and learn to be humble.

I express my gratitude to all my teachers whose teaching have brought me to this stage of academic zenith, in particular, I want to acknowledge my profound gratitude to my kind natured, eminent and highly devoted supervisor, **Dr. Zaheer Abbas**, who aided me with many inspirational discussions. His many valuable expertise, comments, suggestions and instructions are most welcome and greatly improved the clarity of this document. I am placing my earnest thanks to **Dr. Zaheer Abbas**.

I am greatly thankful to **Dr. Irshad Ahmad Arshad** (*Chairman, Department of Mathematics and Statistics, IUI*) who always provide me full opportunities and affectionate help to complete my MS research work. My very special thanks are due to my highly devoted and respected teachers **Dr. Tariq Javed** and **Dr. Nasir Ali** for their complete support in the achievement of my task.

I am highly grateful to my affectionate and candid teacher **Mr. Tahir Mehmood** who blessed me with his precious guidance and always help me in every difficult moment throughout my educational carrier. I pay my sincere thanks to **Dr. Matloob Anwar, Dr. Muhammad Sajid, Mr. Aamir Nadeem** and my elder brother **Mr. Aurang Zaib**, who provided me emotional support and future motivation in the whole journey of this research work.

I express my deepest sense of gratitude to my **parents, brothers, sisters** and my **family**, who is always real pillars for my encouragement and showered their everlasting love, care and support throughout my life. Their humble prayers have always been a source of great inspiration for me and whose sustained hope led myself to where, I am today.

I would also like to thank all my **friends** like **Shahid, Zaheer, Arshad, shafiq, Mohsin, Abid, Nadeem, Tasleem** and others who directly or indirectly helped me during my MS period.

Noor Muhammad

July, 14, 2011.

Preface

The boundary layer flow and heat transfer due to a continuous stretching surface are important from theoretical as well as practical point of view because of their wide applications in polymer technology and engineering processes. In particular, in the extrusion of a polymer in a melt-spinning process, the extrudate from the die is generally drawn and simultaneously stretched into a thin sheet, the boundary layer along material handling conveyers, the aerodynamic extrusion of plastic sheets, glass blowing, paper production, the boundary layer along a liquid film in the condensation process and many others. After the pioneering work of Sakiadis [1, 2], various aspects of the problem have been discussed by many researchers. Crane [3] discussed the flow of a viscous fluid over a linearly stretching surface. However, to the best of our knowledge, first Wang [4] has been studied the flow of liquid film on an unsteady stretching sheet. Andersson et al. [5] investigated the heat transfer in a liquid film over an unsteady stretching sheet. Recently, Elbashbeshy and Bazid [6] have presented the similarity solution of boundary layer flow and heat transfer due to an unsteady stretching sheet. After the work of [6], many authors have investigated various aspects of this problem and obtained similarity solution, e.g. [7-11]. Having in mind all the stated motivations above, the present dissertation is arranged as follow:

Chapter one aims to present some basic definitions and flow equations. Concepts of boundary flow, the homotopy analysis method and shooting method also included.

Chapter two deals the boundary layer flow and heat transfer due to an unsteady stretching sheet. The governing time-dependent equations are transformed to ordinary differential equations using similarity transformations. The system of ordinary differential equations is solved numerically using shooting method with Runge-Kutta scheme. The effects of various governing parameters on the velocity and temperature fields are studied. In fact this chapter is a review of the work done by Elbashbeshy and Bazid [6].

Chapter three aims to extend the work of [6] into four directions: (i) to consider the magnetic field (ii) to analyze the flow in a porous medium (iii) to consider the stagnation-point flow and (iv) to include the effects of slip condition. The governing non-linear partial differential equations are converted into non-linear ordinary differential equations by employing similarity transformations. This system has been solved both analytically using homotopy analysis method (HAM) and numerically using shooting method with Runge-Kutta scheme. The influences of sundry parameters on the dimensionless velocity and temperature fields are shown through graphs. The numerical values of skin-friction coefficient and local Nusselt number for various parameters are also given in tabular form. The comparison of both solutions are given and found in excellent agreement.

Contents

1 Basic definitions and equations	3
1.1 Flow	3
1.2 Fluid	3
1.3 Types of Flow	3
1.3.1 Uniform flow	3
1.3.2 Non-uniform flow	3
1.3.3 Steady flow	4
1.3.4 Unsteady flow	4
1.3.5 Compressible flow	4
1.3.6 Incompressible flow	4
1.4 Classification of fluids	4
1.5 Miscellaneous	6
1.5.1 Porous medium	6
1.5.2 Boundary layer equations	6
1.5.3 Stagnation point	9
1.5.4 Slip condition	9
1.5.5 Maxwell's equations	9
1.6 Governing Equations	10
1.6.1 Equation of continuity	10
1.6.2 Equation of motion	10
1.6.3 Energy equation	11
1.7 Solution techniques	11

1.7.1	Runge-Kutta Method	11
1.7.2	Shooting Method	12
1.7.3	Homotopy Analysis Method (HAM)	14
2	Heat transfer over an unsteady stretching sheet	16
2.1	Introduction	16
2.2	Governing Equations	16
2.3	Solution	18
2.4	Results and discussion	19
3	MHD stagnation slip flow over an unsteady stretching surface in porous medium	23
3.1	Introduction	23
3.2	Flow equations	24
3.3	Solution of the problem	26
3.3.1	Numerical solution	26
3.3.2	Homotopy analysis solution	27
3.3.3	Convergence of the HAM solution	30
3.4	Results and discussion	32

Chapter 1

Basic definitions and equations

The aim of this chapter is to provide some basic definitions and governing equations which are used to discuss the motion of fluid. The basic concepts of the solution techniques are also given.

1.1 Flow

A material or substance goes under deformation when certain forces act upon it. If the deformation exceed continuously with out limit, then the phenomena is known as flow.

1.2 Fluid

A fluid is a material/substance that continuously deforms (flows) under an applied shear (tangential) stress.

1.3 Types of Flow

1.3.1 Uniform flow

A flow in which the velocity of fluid particles are same at each point.

1.3.2 Non-uniform flow

A flow in which the velocity of fluid particles are different at different point.

1.3.3 Steady flow

It is a flow in which fluid properties does not depend on the time 't'. Mathematically, it is defined as

$$\frac{\partial \xi}{\partial t} = 0, \quad (1.1)$$

where ξ is fluid property.

1.3.4 Unsteady flow

It is a flow in which fluid properties depend on the time 't', i.e.,

$$\frac{\partial \xi}{\partial t} \neq 0, \quad (1.2)$$

where ξ is any fluid property.

1.3.5 Compressible flow

A flow in which the density of the fluid is not constant, is called compressible flow. It is denoted by symbol ' ρ '. Mathematically, it is given by

$$\rho = \frac{m}{v}. \quad (1.3)$$

1.3.6 Incompressible flow

A flow in which the density of the fluid is constant throughout the flow is called incompressible flow.

1.4 Classification of fluids

There are two main types of fluids.

(i) Ideal fluids

(ii) Real fluids

(i) Ideal fluids

A fluid which has zero viscosity is called an ideal fluid. i.e. a fluid in which there is no friction. All ideal fluids are incompressible. Mineral water is an example of an ideal fluid.

(ii) Real fluids

A fluid for which the viscosity is not equal to zero is known as real fluid.

$$\mu \neq 0. \quad (1.4)$$

Real fluids are also known as viscous fluids. Real fluids are further divided into two main classes.

(a) Newtonian fluids

All the fluids which satisfy the Newton's law of viscosity are called Newtonian fluids. The Newtonian's law of viscosity is stated as "shear stress is directly and linearly proportional to the rate of deformation". Mathematically, it is stated as

$$\tau_{xy} = \mu \left(\frac{du}{dy} \right). \quad (1.5)$$

where μ is absolute viscosity, τ_{xy} is shear stress and du/dy is the shear rate. Examples of Newtonian fluids are water, air, gasoline etc.

(b) Non-Newtonian fluids

All fluids which do not satisfy the Newton's law of viscosity are called non-Newtonian fluids. Such types of fluids obey the power law model, in which shear stress is directly but non-linearly proportional to the rate of deformation. Mathematically,

$$\tau_{xy} \propto \left(\frac{du}{dy} \right)^n, \quad n \neq 1. \quad (1.6)$$

$$\tau_{xy} = k \left(\frac{du}{dy} \right)^n. \quad (1.7)$$

where n is the flow behavior index and k is the consistency index. Examples of Non-Newtonian fluids are shampoo, gel, soap and blood etc. The above equation can be rewritten in the form

$$\tau = k \left| \frac{du}{dy} \right|^{n-1} \frac{du}{dy} = \eta^* \frac{du}{dy} \quad (1.8)$$

The coefficient $\eta^* = k |du/dy|^{n-1}$ is called as the apparent viscosity.

1.5 Miscellaneous

1.5.1 Porous medium

A porous medium is a material containing pores. The pores are typically filled with a fluid like liquid or gas. The skeletal material is usually a solid, but structures like foams are analyzed using concept of porous media. A porous medium is characterized by its porosity. Many natural substances like rocks, soil, bones, wood and man made material such as cements are considered as porous media. Porous is that type of medium of flow in which we see suction and injection measured.

A porous medium has many practical applications in science and engineering like filtration, petroleum engineering, geology and different branches of mechanics.

1.5.2 Boundary layer equations

A major contribution to the study of fluid mechanics was initiated L. Prandtl in the year 1901. He described to classify the essence and influence of viscosity in flows at high Reynolds numbers and he showed how the Navier-Stokes equations could be simplified to provide approximate solutions under this situation. A boundary layer flow deals with that portion of a fluid flow, near a solid surface, where shear stresses are of significance and the inviscid-flow assumption is not a reliable assumption. A solid surface has interaction with a viscous fluid flow. This is due to the no-slip condition which is a physical requirement that the fluid and solid have equal velocities at their interface. Therefore a fluid flow is retarded by a fixed solid surface and a finite slow-moving boundary layer is formed. A requirement that the boundary layer be thin is for the Reynolds number of the body to be large, i.e. 10^3 or greater. Under the said conditions;

the flow outside the boundary layer is largely inviscid and plays the role of a driving mechanism for the layer.

The discovery of the boundary layer equations can be considered as one of the more important advances in fluids. The use of an order of magnitude analysis results in the governing Navier–Stokes equations of viscous fluid flow to be immensely simplified within the boundary layer. Indeed, the partial differential equations (PDEs) becomes parabolic. This greatly enhances the solution procedure for the equations. The flow is divided into an inviscid portion (which is easy to solve by a number of approaches) and the boundary layer (which is governed by an easier to solve PDE). Navier–Stokes equations for an incompressible two-dimensional flow are

$$u \frac{\partial u}{\partial x} + v \frac{\partial u}{\partial y} = -\frac{1}{\rho} \frac{\partial p}{\partial x} + \nu \left(\frac{\partial^2 u}{\partial x^2} + \frac{\partial^2 u}{\partial y^2} \right), \quad (1.9)$$

$$u \frac{\partial v}{\partial x} + v \frac{\partial v}{\partial y} = -\frac{1}{\rho} \frac{\partial p}{\partial y} + \nu \left(\frac{\partial^2 v}{\partial x^2} + \frac{\partial^2 v}{\partial y^2} \right), \quad (1.10)$$

$$\frac{\partial u}{\partial x} + \frac{\partial v}{\partial y} = 0. \quad (1.11)$$

In above expressions ν is the kinematic viscosity, ρ is the density of the fluid, p is the pressure, x and y are the horizontal and vertical coordinates and u and v the velocity components parallel to x and y axes. A wall is considered $y = 0$. The non-dimensional quantities are defined as

$$x^* = \frac{x}{L}, \quad y^* = \frac{y}{\delta_1}, \quad u^* = \frac{u}{U}, \quad v^* = \frac{v}{U} \frac{L}{\delta_1}, \quad p^* = \frac{p}{\rho U^2}. \quad (1.12)$$

Here L indicates the horizontal length scale and δ_1 the boundary layer thickness. Equations (1.9) to (1.11) in non-dimensional variables are

$$u^* \frac{\partial u^*}{\partial x^*} + v^* \frac{\partial u^*}{\partial y^*} = -\frac{\partial p^*}{\partial x^*} + \frac{\nu}{UL} \frac{\partial^2 u^*}{\partial x^{*2}} + \frac{\nu}{UL} \left(\frac{L}{\delta_1} \right)^2 \frac{\partial^2 u^*}{\partial y^{*2}}, \quad (1.13)$$

$$u^* \frac{\partial v^*}{\partial x^*} + v^* \frac{\partial v^*}{\partial y^*} = -\left(\frac{L}{\delta_1} \right)^2 \frac{\partial p^*}{\partial y^*} + \frac{\nu}{UL} \frac{\partial^2 v^*}{\partial x^{*2}} + \frac{\nu}{UL} \left(\frac{L}{\delta_1} \right)^2 \frac{\partial^2 v^*}{\partial y^{*2}}, \quad (1.14)$$

$$\frac{\partial u^*}{\partial x^*} + \frac{\partial v^*}{\partial y^*} = 0, \quad (1.15)$$

in which the Reynold number is written as

$$R = \frac{UL}{\nu}. \quad (1.16)$$

The inertial and viscous forces are of the same order and hence

$$\frac{\nu}{UL} \left(\frac{L}{\delta_1} \right)^2 = O(1) \quad (1.17)$$

or

$$\delta_1 = O\left(R^{-1/2}L\right). \quad (1.18)$$

Dropping asterisks and utilizing above equation one obtains

$$u \frac{\partial u}{\partial x} + v \frac{\partial u}{\partial y} = -\frac{\partial p}{\partial x} + \frac{1}{R} \frac{\partial^2 u}{\partial x^2} + \frac{\partial^2 u}{\partial y^2}, \quad (1.19)$$

$$\frac{1}{R} \left(u \frac{\partial v}{\partial x} + v \frac{\partial v}{\partial y} \right) = -\frac{\partial p}{\partial y} + \frac{1}{R^2} \left(\frac{\partial^2 v}{\partial x^2} + \frac{\partial^2 v}{\partial y^2} \right), \quad (1.20)$$

$$\frac{\partial u}{\partial x} + \frac{\partial v}{\partial y} = 0. \quad (1.21)$$

For $R \rightarrow \infty$ we have

$$u \frac{\partial u}{\partial x} + v \frac{\partial u}{\partial y} = -\frac{\partial p}{\partial x} + \frac{\partial^2 u}{\partial y^2}, \quad (1.22)$$

$$-\frac{\partial p}{\partial y} = 0. \quad (1.23)$$

$$\frac{\partial u}{\partial x} + \frac{\partial v}{\partial y} = 0. \quad (1.24)$$

in which Eq. (1.23) shows that pressure is constant across the boundary layer. In dimensional form, Eqs. (1.22) to (1.24) become

$$u \frac{\partial u}{\partial x} + v \frac{\partial u}{\partial y} = -\frac{1}{\rho} \frac{\partial p}{\partial x} + \nu \frac{\partial^2 u}{\partial y^2}, \quad (1.25)$$

$$-\frac{1}{\rho} \frac{\partial p}{\partial y} = 0, \quad (1.26)$$

$$\frac{\partial u}{\partial x} + \frac{\partial v}{\partial y} = 0. \quad (1.27)$$

1.5.3 Stagnation point

The boundary layer has the point in the flow field where the streamlines of the fluid takes different directions around that point. that point is called stagnation point. At stagnation point the local velocity of the fluid is zero.

1.5.4 Slip condition

If the velocity of the fluid in contact with the boundary of the surface is not same as that of boundary, we use slip condition. The difference of the velocities between fluid and boundary may have different relations like linear, quadratic, cubic, parabolic, hyperbolic etc.

1.5.5 Maxwell's equations

Maxwell's equations are the set of four equations which relate the electric and magnetic field to their sources, charge density and current density. Individually, these equations are known as *Gauss's law*, *Gauss's law for magnetism*, *Faraday's law of induction* and *Ampere's law with Maxwell's correction*. These equations are described as

$$\nabla \cdot \mathbf{E} = \frac{\rho}{\epsilon_0}, \quad (1.28)$$

$$\nabla \cdot \mathbf{B} = 0, \quad (1.29)$$

$$\nabla \times \mathbf{E} = -\frac{\partial \mathbf{B}}{\partial t}, \quad (1.30)$$

$$\nabla \times \mathbf{B} = \mu_0 \mathbf{J} + \mu_0 \epsilon_0 \frac{\partial \mathbf{E}}{\partial t}. \quad (1.31)$$

In the above equations ϵ_0 is the permittivity of the free space also called electric constant, μ_0 is the permeability of free space which is also called magnetic constant, ρ is the total charge density and \mathbf{J} is the total current density. The total magnetic field is $\mathbf{B} = (B_0 + \mathbf{b})$, where \mathbf{b} is induced magnetic field. By *Ohm's law* in generalized form we have

$$\mathbf{J} = \sigma (\mathbf{E} + \mathbf{V} \times \mathbf{B}), \quad (1.32)$$

where σ is the electric conductivity of the fluid. In the present case there is no applied electric field, also the induced magnetic field is neglected due to the assumption of low magnetic Reynold number. Therefore, the Lorentz force in the direction of the flow becomes

$$(\mathbf{J} \times \mathbf{B}) = -\sigma B_0^2 V, \quad (1.33)$$

where B_0 is the applied magnetic field and V is the velocity.

1.6 Governing Equations

1.6.1 Equation of continuity

The mathematical relation of conservation of mass for fluids is known as equation of continuity. It has the following form

$$\frac{\partial \rho}{\partial t} + \nabla \cdot (\rho \mathbf{V}) = 0, \quad (1.34)$$

and for an incompressible fluid it reduces to

$$\nabla \cdot \mathbf{V} = 0.$$

1.6.2 Equation of motion

The motion of fluid is governed by law of conservation of momentum. The application of this law to an arbitrary control volume in flowing fluid yield the following equation commonly known an equation of motion.

$$\rho \frac{d\mathbf{V}}{dt} = -\nabla p + \text{div } \mathbf{T} + \rho \mathbf{b}. \quad (1.35)$$

In above equation \mathbf{T} is Cauchy stress tensor and \mathbf{b} is body force per unit mass.

1.6.3 Energy equation

Energy in a system may take on various forms (e.g. kinetic, potential, heat, light). Mathematical form of energy equation is described as

$$\rho c_p \frac{D\theta}{Dt} = \mathbf{T} \cdot \mathbf{L} - \nabla \cdot \mathbf{q}, \quad (1.36)$$

in which

$$\mathbf{L} = \nabla \mathbf{V}. \quad (1.37)$$

Energy equation also represents the 'Law of Conservation of Energy'.

1.7 Solution techniques

1.7.1 Runge-Kutta Method

There are many different schemes for solving initial value problems relating to ordinary differential equations numerically, but due to highest order of accuracy i.e. of $O(4)$ we prefer to use the Runge-Kutta method.

The general equation of second order of initial value problem can be written as

$$\frac{d^2y}{dx^2} = f\left(x, y, \frac{dy}{dx}\right), \quad (1.38)$$

subject to initial conditions

$$y(x_0) = y_0, \quad \frac{dy}{dx}(x_0) = a. \quad (1.39)$$

In order to solve the problem, we need to convert second order initial value problem to the system of first order initial value problem by defining

$$\frac{dy}{dx} = z = g(x, y, z). \quad (1.40)$$

so we will have

$$\frac{dz}{dx} = f(x, y, z), \quad (1.41)$$

with initial conditions

$$y(x_0) = y_0, \quad z(x_0) = a. \quad (1.42)$$

Now the Runge-Kutta method of order 4 for the above system of first order differential Eqs. (1.40) and (1.41) is defined as

$$y_{n+1} = y_n + \frac{1}{6} (k_1 + 2k_2 + 2k_3 + k_4), \quad (1.43)$$

and

$$z_{n+1} = z_n + \frac{1}{6} (l_1 + 2l_2 + 2l_3 + l_4), \quad (1.44)$$

where

$$k_1 = hg(x_n, y_n, z_n), \quad l_1 = hf(x_n, y_n, z_n), \quad (1.45)$$

$$k_2 = hg\left(x_n + \frac{h}{2}, y_n + \frac{k_1}{2}, z_n + \frac{l_1}{2}\right), \quad l_2 = hf\left(x_n + \frac{h}{2}, y_n + \frac{k_1}{2}, z_n + \frac{l_1}{2}\right) \quad (1.46)$$

$$k_3 = hg\left(x_n + \frac{h}{2}, y_n + \frac{k_2}{2}, z_n + \frac{l_2}{2}\right), \quad l_3 = hf\left(x_n + \frac{h}{2}, y_n + \frac{k_2}{2}, z_n + \frac{l_2}{2}\right) \quad (1.47)$$

$$k_4 = hg(x_n + h, y_n + k_3, z_n + l_3), \quad l_4 = hf(x_n + h, y_n + k_3, z_n + l_3) \quad (1.48)$$

where h is uniform step size defined as

$$h = \frac{x_n - x_0}{n}, \quad (1.49)$$

n is number of step.

1.7.2 Shooting Method

Shooting method is an iterative technique which is very popular for the two points boundary value problems. In this technique, the boundary value problem of higher order is first reduced to the system of first order initial value problem by letting the missing condition. Then our goal is to find the solution of initial value problem instead of given boundary value problem directly. For this purpose, any scheme for the solution of initial value problem can be used. Runge-Kutta method of order 4 is used for this purpose. For illustration, lets consider a second

order boundary value problem

$$\frac{d^2y}{dx^2} = f\left(x, y, \frac{dy}{dx}\right). \quad (1.50)$$

with boundary conditions

$$y(0) = 0, \quad y(L) = A1, \quad (1.51)$$

where f is arbitrary function and data is prescribed at $x = 0$ and $x = L$. The same differential equation describes an initial value problem if data is prescribed as

$$y(0) = 0, \quad y'(0) = s. \quad (1.52)$$

To solve the boundary value problem we reduce it into a system of two first order differential equations as

$$\frac{dy}{dx} = u, \quad \frac{du}{dx} = f(x, y, u), \quad (1.53)$$

with initial conditions

$$y(0) = 0, \quad y'(0) = u(0) = s, \quad (1.54)$$

where 's' denotes the missing initial conditions which will be assigned an initial value. Next we will find the actual value of 's' such that the solution of Eq. (1.50) subject to the initial conditions (1.52) satisfies the boundary conditions (1.51). In other words, if the solutions of the initial value problems are denoted by $y(x, s)$ and $u(x, s)$, one searches for the value of 's' such that

$$y(L, s) - A1 = 0 = \phi(s) \quad (\text{say}). \quad (1.55)$$

Here Newton's formula can be used to find the value of 's' as we are to choose a roots of linear algebraic Eq. (1.53), which is given as

$$s^{(n+1)} = s^{(n)} - \frac{\phi(s^{(n)})}{\frac{d\phi}{ds}(s^{(n)})}. \quad (1.56)$$

which implies that

$$s^{(n+1)} = s^{(n)} - \frac{y(L, s^{(n)}) - A1}{\frac{\partial y}{\partial s}(L, s^{(n)})}. \quad (1.57)$$

To find the derivative of y with respect to ' s ' Eqs. (1.53) and (1.54) are differentiated with respect to ' s ' and we get

$$\frac{dY}{dx} = U, \quad \frac{dU}{dx} = \frac{\partial f}{\partial y} Y + \frac{\partial f}{\partial u} U, \quad (1.58)$$

where

$$Y = \frac{\partial y}{\partial s}, \quad U = \frac{\partial u}{\partial s}, \quad (1.59)$$

and initial conditions take the following form

$$Y(0) = 0, \quad U(0) = 1. \quad (1.60)$$

1.7.3 Homotopy Analysis Method (HAM)

The homotopy analysis method (HAM) is developed by Liao [12, 13] in 1992. It is a powerful analytical technique to solve the non-linear boundary value problems. Many researches [14–25] have been applied this technique successfully to solve the non-linear equations. Here we give a simple example to solve the application of homotopy analytical method (HAM).

The idea of the homotopy is very simple and straightforward. For example, consider a differential equation

$$\mathcal{N}[u(t)] = 0, \quad (1.61)$$

where \mathcal{N} is a nonlinear operator, t denotes the time, and $u(t)$ is an unknown variable. In the initial step we suppose $u_0(t)$ as an initial approximation of $u(t)$ and \mathcal{L} as auxiliary linear operator with the property

$$\mathcal{L}(f) = 0, \text{ when } f = 0. \quad (1.62)$$

We then construct the zeroth order deformation equation as

$$\mathcal{H}[\phi(t, q); q] = (1 - q)\mathcal{L}[\phi(t, q) - u_0(t)] + q[\mathcal{N}[\phi(t, q)]] = 0. \quad (1.63)$$

where $q \in [0, 1]$ is an embedding parameter and $\phi(t, q)$ is a function of t and $q = 1$, we have

$$\mathcal{H}[\phi(t, q) \cdot q]|_{q=0} = \mathcal{L}[\phi(t, 0) - u_0(t)], \quad (1.64)$$

and

$$\mathcal{H}[\phi(t, q) \cdot q]|_{q=1} = \mathcal{N}[\phi(t, 1)]. \quad (1.65)$$

Clearly it shows that if we use this in Eq. (1.63) we get

$$\phi(t, 0) = u_0(t),$$

is the solution of the equation

$$\mathcal{H}[\phi(t, q) \cdot q]|_{q=0} = 0. \quad (1.66)$$

and

$$\phi(t, 1) = u(t),$$

is therefore obviously the solution of the equation

$$\mathcal{H}[\phi(t, q) \cdot q]|_{q=1} = 0. \quad (1.67)$$

It implies that as the embedding parameter q increases from 0 to 1, the solution $\phi(t, q)$ of the equation (1.67), varies from $u_0(t)$ to the final solution $u(t)$.

Chapter 2

Heat transfer over an unsteady stretching sheet

2.1 Introduction

This chapter deals the similarity solution of laminar flow and heat transfer due to an unsteady stretching surface. The governing non-linear partial differential equations are transformed to non-linear ordinary differential equations using the similarity transformations. The system of non-linear ordinary differential equations are solved numerically using shooting method with Runge-Kutta algorithm. The effects of various parameters on the velocity and temperature profiles are discussed through tables and graphs. This chapter is a review of the paper by Elbashbeshy and Bazid [6].

2.2 Governing Equations

Consider the two-dimensional unsteady flow of an incompressible viscous fluid over an unsteady stretching sheet. The x -axis is taken along the direction of the sheet, while the y -axis is perpendicular to it. At time $t = 0$, the sheet is stretched with the velocity $U_w = bx/1 - \delta t$ (where b is stretching rate and δ is positive constant). The surface temperature is T_w and the ambient fluid temperature is T_∞ , where $T_w > T_\infty$. The boundary layer equations for the flow

and energy are given as:

$$\frac{\partial u}{\partial x} + \frac{\partial v}{\partial y} = 0. \quad (2.1)$$

$$\frac{\partial u}{\partial t} + u \frac{\partial u}{\partial x} + v \frac{\partial u}{\partial y} = \nu \frac{\partial^2 u}{\partial y^2}, \quad (2.2)$$

$$\frac{\partial T}{\partial t} + u \frac{\partial T}{\partial x} + v \frac{\partial T}{\partial y} = \alpha \frac{\partial^2 T}{\partial y^2}, \quad (2.3)$$

where u and v are the velocity components in the x - and y - axis directions, respectively. ν is kinematic viscosity. α is thermal diffusivity and T is the temperature of the fluid.

The corresponding boundary conditions are

$$u = U_w(x, t) = \frac{bx}{1 - \delta t}, \quad v = 0, \quad T = T_w(x, t) = T_\infty + \frac{cx}{\nu(1 - \delta t)} \quad \text{at } y = 0, \quad (2.4)$$

$$u \rightarrow 0, \quad T \rightarrow T_\infty \quad \text{as } y \rightarrow \infty, \quad (2.5)$$

where b , c and δ are constants with $b \geq 0$, $c \geq 0$ and $\delta > 0$ ($\delta t < 1$), and both b and c have dimension time^{-1} .

The continuity equation is satisfied by introducing a stream function $\psi(x, y)$ as

$$u = \frac{\partial \psi}{\partial y}, \quad v = -\frac{\partial \psi}{\partial x}. \quad (2.6)$$

To simplify the flow equations, we use the following dimensionless quantities

$$\eta = \sqrt{\frac{b}{\nu(1 - \delta t)}} y, \quad \psi(x, y) = \sqrt{\frac{\nu b}{(1 - \delta t)}} x f(\eta), \quad (2.7)$$

$$\theta(\eta) = \frac{T - T_\infty}{T_w - T_\infty}, \quad T_w - T_\infty = \frac{bx^2}{2\nu} (1 - \delta t)^{\frac{3}{2}}. \quad (2.8)$$

Using Eq. (2.7) and (2.8), Eqs. (2.2) and (2.3) become

$$f''' + f f'' - f'^2 - A \left(f' + \frac{1}{2} \eta f'' \right) = 0, \quad (2.9)$$

$$\text{Pr} \theta'' - 2f'\theta + f\theta' - \frac{A}{2} (3\theta + \eta\theta') = 0, \quad (2.10)$$

and boundary conditions are

$$f = 0, f' = 1, \theta = 1 \text{ at } \eta = 0. \quad (2.11)$$

$$f' \rightarrow 0, \theta \rightarrow 0 \text{ as } \eta \rightarrow \infty, \quad (2.12)$$

where $A = \delta/b$ is the unsteadiness parameter and $\text{Pr} = \nu/\alpha$ is the Prandtl number.

It should be mentioned here that in the paper of Elbashbeshy and Bazid the sign of the term $2f'\theta$ is positive in their energy equation due to the incorrect definition of $\Delta T = T_w - T_\infty$ and hence an exact comparison is not possible. According to them $\Delta T = T_w - T_\infty = \frac{b}{2\nu A^2}(1 - \delta t)^{-\frac{3}{2}}$ but the correct value is $\frac{bx^2}{2\nu}(1 - \delta t)^{-\frac{3}{2}}$. Due to this error, some physically unrealistic phenomena in the velocity and temperature fields are encountered for specific values of the unsteadiness parameter. Mohamed Abd El-Aziz also mentioned this error in his paper [10].

The skin-friction coefficient C_f and the local Nusselt number Nu_x are given by

$$C_f = \frac{\tau_w}{\rho U_w^2}, \quad Nu_x = \frac{xq_w}{k_m(T_w - T_\infty)}, \quad (2.13)$$

where k_m is thermal conductivity, τ_w is the shear stress at the wall and q_w is the heat flux at wall, which are define as

$$\tau_w = \mu \left(\frac{\partial u}{\partial y} \right)_{y=0}, \quad \text{and } q_w = -k_m \left(\frac{\partial T}{\partial y} \right)_{y=0}. \quad (2.14)$$

With the help of Eqs. (2.7 – 2.8) and (2.14), Eq. (2.13) yields

$$\frac{Nu_x}{\sqrt{Re_x}} = -\theta'(0), \quad \text{or } \sqrt{Re_x} C_f = f''(0). \quad (2.15)$$

where and $Re_x = xU_w/\nu$ is the local Reynolds number.

2.3 Solution

To find the numerical solution, we use the most effective shooting method with fourth order Runge-Kutta integration scheme. The non-linear equations (2.9) and (2.10) with the boundary

conditions (2.11) and (2.12) are transformed into a system of five first order differential equations as follows:

$$\frac{df_0}{d\eta} = f_1,$$

$$\frac{df_1}{d\eta} = f_2,$$

$$\frac{df_2}{d\eta} = -f f_2 + (f_1)^2 + A f_1 + \frac{1}{2} A \eta f_2,$$

$$\frac{d\theta_0}{d\eta} = \theta_1,$$

$$\frac{d\theta_1}{d\eta} = \text{Pr} \left(2f_1\theta - f\theta_1 + \frac{3}{2}A\theta + \frac{1}{2}A\eta\theta_1 \right),$$

and the boundary conditions are

$$f(0) = 0, f_1(0) = 1, f_1(\infty) = 0,$$

$$\theta(0) = 1, \theta(\infty) = 0.$$

Here $f_0 = f(\eta)$ and $\theta_0 = \theta(\eta)$. A boundary value problem is first converted into an initial value problem by appropriately guessing the missing conditions $f_2(0)$ and $\theta_1(0)$. The resultant initial value problem is solved by shooting method for a set of parameters appearing in the governing equations with a known values of $f_2(0)$ and $\theta_1(0)$.

2.4 Results and discussion

Figs. (2.1) – (2.4) are plotted in order to see the effects of the involving parameters on the velocity and temperature profiles. The numerical values of the skin friction coefficient and the local Nusselt number for different values of physical parameters are also given in Table 2.1.

Table 2.1: Numerical values of $-\theta'(0)$ and $-f''(0)$ for various values of Prandtl number Pr and unsteadiness parameter A .

Pr \ A	0		0.8		1.2		2.0	
	$-\theta'(0)$	$-f''(0)$	$-\theta'(0)$	$-f''(0)$	$-\theta'(0)$	$-f''(0)$	$-\theta'(0)$	$-f''(0)$
0.01	0.0294284	1.0014	0.202712	1.26106	0.239185	1.37774	0.27583	1.58738
0.1	0.263474	1.0014	0.453578	1.26106	0.503033	1.37774	0.60478	1.58738
1.0	1.33889	1.0014	1.67209	1.26106	1.81793	1.37774	2.07817	1.58738
10.0	4.76411	1.0014	5.70494	1.26106	6.12013	1.37774	6.88176	1.58738

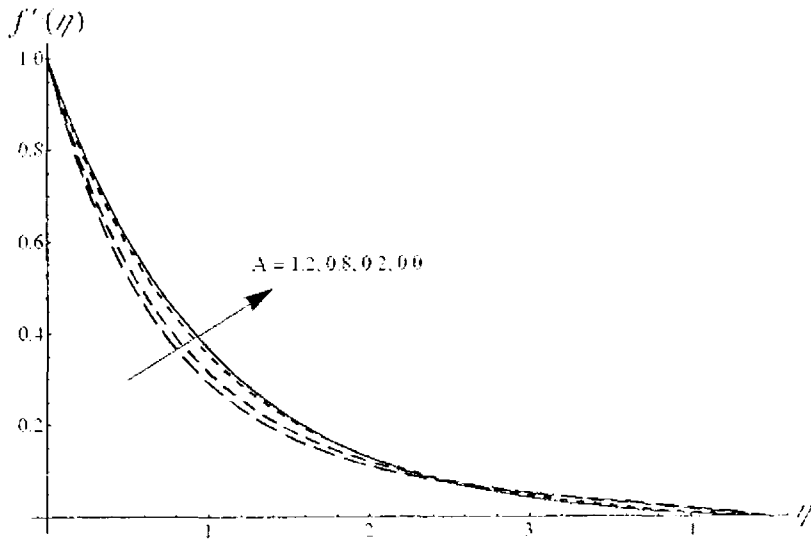


Fig. 2.1: Velocity profile $f'(\eta)$ against η for various values of A .

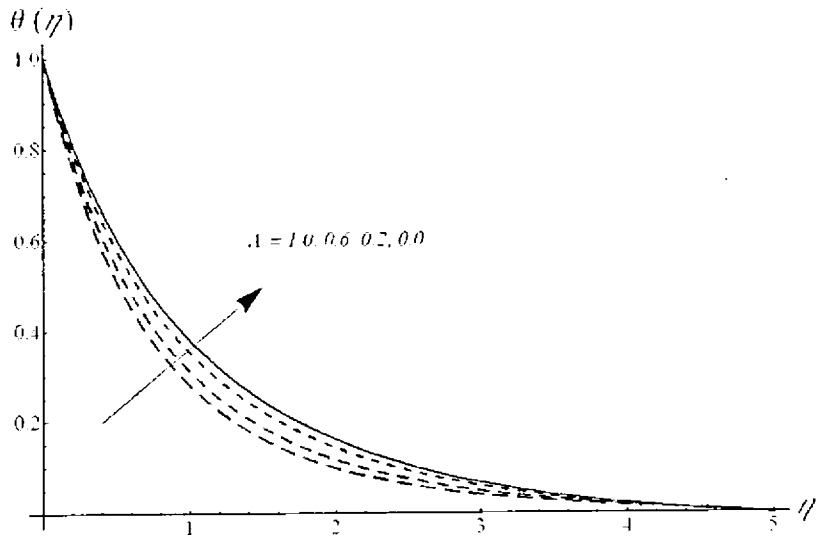


Fig. 2.2: Temperature profile $\theta(\eta)$ against η for various values of A .

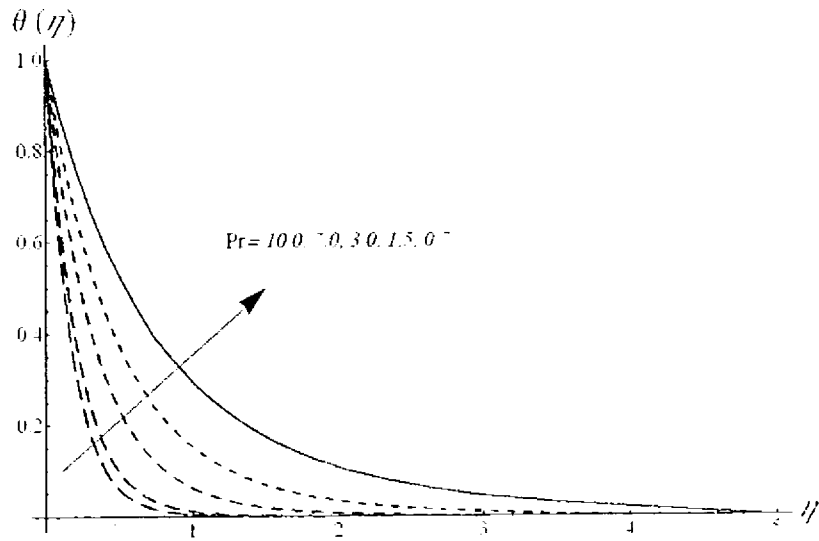


Fig. 2.3: Temperature profile $\theta(\eta)$ against η for various values of Pr

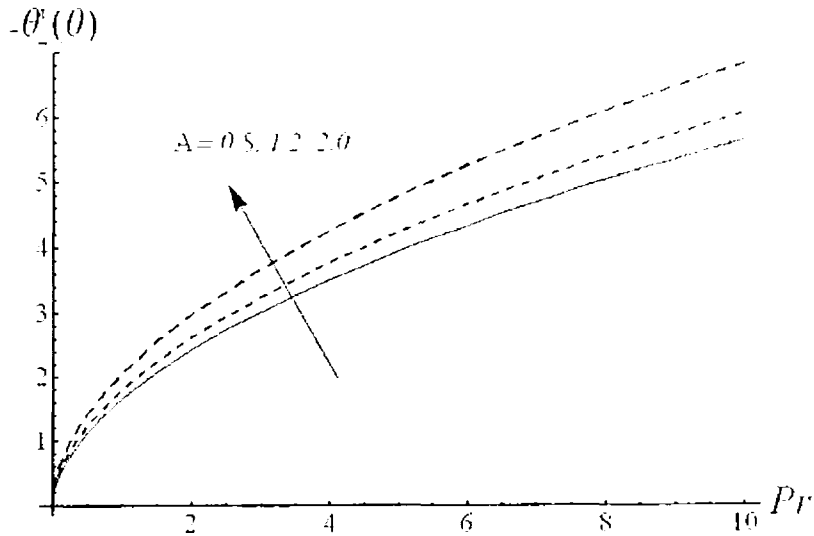


Fig. 2.4: Variation of heat transfer coefficient $-\theta'(0)$ against Pr for different values of A .

Table 1 gives the numerical values of the skin-friction coefficient $-f''(0)$ and the local Nusselt number $-\theta'(0)$ for different values of Pr and A . It is found that the magnitude of $-\theta'(0)$ is increased by increasing the values of Pr , and the magnitude of $-f''(0)$ also increases for large values of A .

Fig. 2.1 shows the effects of an unsteadiness parameter A on the velocity component $f'(\eta)$. It is noted that the velocity decreases by increasing the values of A . The boundary layer thickness also decreases as A increases. Fig. 2.2 gives the variations of an unsteadiness parameter A on the temperature fields $\theta(\eta)$. Both the temperature and the thermal boundary layer thickness decrease for large values of A . The change in the temperature field $\theta(\eta)$ for different values of Prandtl number Pr can be seen from Fig. 2.3. It is observed that the temperature decreases by increasing the values of Pr . It is also noted that the thermal boundary layer thickness decreases as the Prandtl number Pr is increased. Fig. 2.4 shows the variations of the rate of heat transfer at the wall $-\theta'(0)$ versus Pr for various values of A . The magnitude of $-\theta'(0)$ is increased for large values of an unsteadiness parameter A .

Chapter 3

MHD stagnation slip flow over an unsteady stretching surface in porous medium

3.1 Introduction

This chapter investigates the heat transfer in a stagnation-point flow of MHD viscous fluid over an unsteady stretching sheet in a porous medium with slip condition. The non-linear partial differential equations govern the flow are transformed to a non-linear ordinary differential equations using similarity transformations. The system of non-linear ordinary differential equations is solved both numerically using shooting method with Runge-Kutta algorithm and analytically using homotopy analysis method (HAM). The physical significance of the involving parameters on the flow and temperature fields are discussed through graphs and tables. The graphical results are compared for both solutions. A comparison of obtained results with the existing literature is also given and found in an excellent agreement. This chapter is an extension of the work done by Elbashbeshy and Bazid [6].

3.2 Flow equations

We consider an unsteady, two-dimensional MHD stagnation point flow of a viscous fluid in a porous medium over an unsteady stretching sheet in the region $y > 0$. The x axis is taken along the surface, while the y -axis is perpendicular to the surface. At time $t = 0$, the surface is stretched with the velocity $U_w(x, t)$ along the x -axis, keeping the origin is fixed. It is also assumed that the fluid is electrically conducting and the magnetic field $B(t)$ is applied in the y -direction. The induced magnetic field is neglected due to a small magnetic Reynolds number assumption, where no external electric field is applied. The velocity of the flow outside the boundary layer is $U_e(x, t)$ and the temperature at the surface is $T_w(x, t)$, where $T_w > T_\infty$, with T_∞ being the temperature of the ambient fluid. Under these assumptions along with the boundary layer approximations, the governing equations for the flow and energy are given as:

$$\frac{\partial u}{\partial x} + \frac{\partial v}{\partial y} = 0, \quad (3.1)$$

$$\frac{\partial u}{\partial t} + u \frac{\partial u}{\partial x} + v \frac{\partial u}{\partial y} = \frac{\partial U_e}{\partial t} + U_e \frac{\partial U_e}{\partial x} + \nu \frac{\partial^2 u}{\partial y^2} + \frac{\sigma B^2(t)}{\rho} (U_e - u) + \frac{\nu \phi}{k(t)} (U_e - u), \quad (3.2)$$

$$\frac{\partial T}{\partial t} + u \frac{\partial T}{\partial x} + v \frac{\partial T}{\partial y} = \alpha \frac{\partial^2 T}{\partial y^2}, \quad (3.3)$$

where σ is the electrical conductivity of the fluid, ϕ is porosity of the medium, α is the thermal diffusivity, t is the time and T is the temperature and $k(t)$ is the permeability of the porous medium. Here we assume $k(t)$ and $B(t)$ are of the form

$$k(t) = k_1(1 - \delta t), \quad B(t) = \frac{B_0}{(1 - \delta t)}, \quad (3.4)$$

where k_1 is the initial permeability and B_0 is the constant magnetic field.

The relevant boundary conditions for the present problem are

$$u = U_w(x, t) + N_1 \nu \frac{\partial u}{\partial y}, \quad v = 0, \quad T = T_w(x, t) + D_1 \frac{\partial T}{\partial y} \quad \text{at} \quad y = 0, \quad (3.5)$$

$$u \rightarrow U_e(x, t), \quad T \rightarrow T_\infty \quad \text{as} \quad y \rightarrow \infty. \quad (3.6)$$

Here

$$U_x = \frac{bx}{1 - \delta t}, \quad U_y = \frac{dx}{1 - \delta t}, \quad T_w(x, t) = T_\infty + \frac{cw}{\nu(1 - \delta t)},$$

where $d \geq 0$ and has dimensions (time)⁻¹. $N_1 = N\sqrt{1 - \delta t}$ is the velocity slip parameter and $D_1 = D\sqrt{1 - \delta t}$ is the thermal slip parameter, both are changed with time, and N, D are the initial values of velocity and thermal slip parameters, having dimension (velocity)⁻¹ and length respectively. The no-slip condition can be obtained for $N = 0$ and $D = 0$, respectively.

We define the following similarity transformations

$$\eta = \sqrt{\frac{b}{\nu}}(1 - \delta t)^{-\frac{1}{2}}y, \quad \psi = \sqrt{b\nu}x(1 - \delta t)^{-\frac{1}{2}}f(\eta), \quad (3.7)$$

$$\theta(\eta) = \frac{T - T_\infty}{T_w - T_\infty}, \quad T_w - T_\infty = \frac{bx^2(1 - \delta t)^{-\frac{3}{2}}}{2\nu}, \quad (3.8)$$

and the stream function $\psi(x, y)$ is defined by $u = \partial\psi/\partial y$ and $v = -\partial\psi/\partial x$, such that the continuity equation (3.1) is automatically satisfied.

Using Eqs.(3.7) and (3.8), the Eqs. (3.2) and (3.3) become

$$f''' - f'^2 + ff'' - A\left(f' + \frac{1}{2}\eta f''\right) + M^2(\epsilon - f') + \lambda(\epsilon - f') + A\epsilon + \epsilon^2 = 0, \quad (3.9)$$

$$\frac{-1}{\text{Pr}}\theta'' - 2f'\theta + f\theta' - \frac{A}{2}(3\theta + \eta\theta'), \quad (3.10)$$

and corresponding boundary conditions are

$$f = 0, \quad f' = 1 + \beta f'', \quad \theta = 1 + \gamma\theta' \quad \text{at} \quad \eta = 0, \quad (3.11)$$

$$f' \rightarrow \epsilon, \quad \theta \rightarrow 0 \quad \text{as} \quad \eta \rightarrow \infty, \quad (3.12)$$

where $A = \delta/b$ is the unsteadiness parameter, $\text{Pr} = \nu/\alpha$ is the Prandtl number, $\epsilon = d/b$ is the ratio of the the external flow rate to the stretching rate, $M^2 = \sigma B_0^2/\rho b$ is the magnetic parameter, $\lambda = \nu\phi/k_1b$ is porosity parameter, $\beta = N\sqrt{b\nu}$ is the velocity slip parameter, $\gamma = D\sqrt{\frac{b}{\nu}}$ is the thermal slip parameter and the primes indicate the differentiation with respect to η . It is worth mentioning that we can recovered the no-slip condition by taking $\beta = 0$ and

$\gamma = 0$. It is also noted that if we take $M = \lambda = \epsilon = \beta = \gamma = 0$ then we obtain the same equations as in (2.9) and (2.10) with boundary conditions (2.11) and (2.12).

The skin-friction coefficient C_f and the local Nusselt number Nu_x are given by

$$C_f = \frac{\tau_w}{\rho U_\omega^2}, \quad Nu_x = \frac{xq_w}{k_m(T_w - T_\infty)}, \quad (3.13)$$

where k_m is thermal conductivity, τ_w is the shear stress at the wall and q_w is the heat flux at wall, which are define as

$$\tau_w = \mu \left(\frac{\partial u}{\partial y} \right)_{y=0}, \quad \text{and} \quad q_w = -k_m \left(\frac{\partial T}{\partial y} \right)_{y=0}. \quad (3.14)$$

With the help of Eqs. (3.7 – 3.8) and (3.14), Eq. (3.13) yields

$$\frac{Nu_x}{\sqrt{Re_x}} = -\theta'(0), \quad \text{or} \quad \sqrt{Re_x} C_f = f''(0), \quad (3.15)$$

where $Re_x = xU_\omega/\nu$ is the local Reynolds number.

3.3 Solution of the problem

3.3.1 Numerical solution

In this chapter the numerical solution is obtained by the same scheme that is used in chapter 2. The non-linear Eqs. (3.9) and (3.10) subject to boundary conditions (3.11) and (3.12) are transformed into a system of five first order differential equations as follows:

$$\begin{aligned} \frac{df_0}{d\eta} &= f_1, \\ \frac{df_1}{d\eta} &= f_2, \\ \frac{df_2}{d\eta} &= -ff_2 + (f_1)^2 + Af_1 + \frac{1}{2}A\eta f_2 - M^2(\epsilon - f_1) - \lambda(\epsilon - f_1) - Ac - c^2, \\ \frac{d\theta_0}{d\eta} &= \theta_1, \\ \frac{d\theta_1}{d\eta} &= Pr \left(2f_1\theta - f\theta_1 + \frac{3}{2}A\theta + \frac{1}{2}A\eta\theta_1 \right), \end{aligned}$$

and the boundary conditions are

$$\begin{aligned} f(0) &= 0, \quad f_1(0) = 1 + \beta f_2(0), \quad f_1(\infty) = \epsilon, \\ \theta(0) &= 1 + \gamma\theta_1(0), \quad \theta(\infty) = 0. \end{aligned}$$

3.3.2 Homotopy analysis solution

For the series solutions of Eqs. (3.9) and (3.10) using homotopy analysis method (HAM), it is straight forward that the velocity and the temperature fields $f(\eta)$ and $\theta(\eta)$ can be expressed by the set of base functions

$$\left\{ \eta^k \exp(-n\eta) \mid k \geq 0, n \geq 0 \right\} \quad (3.16)$$

in the form

$$f(\eta) = a_{0,0}^0 + \sum_{n=0}^{\infty} \sum_{k=0}^{\infty} a_{m,n}^k \eta^k \exp(-n\eta), \quad (3.17)$$

$$\theta(\eta) = \sum_{n=0}^{\infty} \sum_{k=0}^{\infty} b_{m,n}^k \eta^k \exp(-n\eta), \quad (3.18)$$

where $a_{m,n}^k$ and $b_{m,n}^k$ are the coefficients. By rule of *solution expressions* of $f(\eta)$ and $\theta(\eta)$, with the help of boundary conditions (3.11) and (3.12) one can choose $f_0(\eta)$ and $\theta_0(\eta)$

$$f_0(\eta) = \epsilon\eta + \frac{(1-\epsilon)(1-e^{-\eta})}{1+\beta}, \quad (3.19)$$

$$\theta_0(\eta) = \frac{e^{-\eta}}{1+\gamma}, \quad (3.20)$$

as the initial guess approximations of $f(\eta)$ and $\theta(\eta)$ and the auxiliary linear operators

$$\mathcal{L}_f(f) = \frac{d^3 f}{d\eta^3} - \frac{df}{d\eta}, \quad (3.21)$$

$$\mathcal{L}_\theta(f) = \frac{d^2 f}{d\eta^2} - f, \quad (3.22)$$

which have the following properties

$$\mathcal{L}_f [C_1 + C_2 \exp(\eta) + C_3 \exp(-\eta)] = 0, \quad (3.23)$$

$$\mathcal{L}_\theta [C_4 \exp(\eta) + C_5 \exp(-\eta)] = 0, \quad (3.24)$$

where C_i , ($i = 1 - 5$) are arbitrary constants. If h_f and h_θ denote the non-zero auxiliary parameters then the zeroth-order deformation problems are constructed as follows:

$$(1 - q) \mathcal{L}_f \left[\widehat{f}(\eta; q) - f_0(\eta) \right] = q h_f \mathcal{N}_f \left[\widehat{f}(\eta; q) \right], \quad (3.25)$$

$$(1 - q) \mathcal{L}_\theta \left[\widehat{\theta}(\eta; q) - \theta_0(\eta) \right] = q h_\theta \mathcal{N}_\theta \left[\widehat{f}(\eta; q), \widehat{\theta}(\eta; q) \right], \quad (3.26)$$

$$\widehat{f}(0; q) = 0, \quad \frac{d\widehat{f}(0, q)}{d\eta} = 1 + \beta \frac{d^2 \widehat{f}(0, q)}{d\eta^2}, \quad \frac{d\widehat{f}(\infty, q)}{d\eta} = \epsilon, \quad (3.27),$$

$$\widehat{\theta}(0, q) = 1 + \gamma \frac{d\widehat{\theta}(0, q)}{d\eta}, \quad \widehat{\theta}(\infty, q) = 0, \quad (3.28)$$

where $q \in [0, 1]$ is an embedding parameter and the nonlinear operators \mathcal{N}_f and \mathcal{N}_θ are

$$\begin{aligned} \mathcal{N}_f \left[\widehat{f}(\eta; q) \right] &= \frac{\partial^3 \widehat{f}(\eta, q)}{\partial \eta^3} - \left(\frac{\partial \widehat{f}(\eta, q)}{\partial \eta} \right)^2 + \widehat{f}(\eta, q) \frac{\partial^2 \widehat{f}(\eta, q)}{\partial \eta^2} - A \frac{\partial \widehat{f}(\eta, q)}{\partial \eta} - \frac{1}{2} A \eta \frac{\partial^2 \widehat{f}(\eta, q)}{\partial \eta^2} \\ &+ M^2 \left(\epsilon - \frac{\partial \widehat{f}(\eta, q)}{\partial \eta} \right) + \lambda \left(\epsilon - \frac{\partial \widehat{f}(\eta, q)}{\partial \eta} \right) + A\epsilon + \epsilon^2, \end{aligned} \quad (3.29)$$

$$\mathcal{N}_\theta \left[\widehat{f}(\eta; q), \widehat{\theta}(\eta; q) \right] = \text{Pr}^{-1} \theta'' - 2 \frac{\partial \widehat{f}(\eta, q)}{\partial \eta} \theta(\eta, q) + f(\eta, q) \frac{\partial \widehat{\theta}(\eta, q)}{\partial \eta} - \frac{3}{2} A \theta(\eta, q) - \frac{1}{2} A \eta \frac{\partial \widehat{\theta}(\eta, q)}{\partial \eta}. \quad (3.30)$$

For $q = 0$ and $q = 1$, the above zeroth-order deformation Eqs. (3.25) and (3.26) have the solutions

$$\widehat{f}(\eta; 0) = f_0(\eta), \quad \widehat{f}(\eta; 1) = f(\eta). \quad (3.31)$$

$$\widehat{\theta}(\eta; 0) = \theta_0(\eta), \quad \widehat{\theta}(\eta; 1) = \theta(\eta). \quad (3.32)$$

Expanding $\widehat{f}(\eta; q)$ and $\widehat{\theta}(\eta; q)$ in Taylor's series with respect to q , we have

$$\widehat{f}(\eta; q) = f_0(\eta) + \sum_{m=1}^{\infty} f_m(\eta) q^m. \quad (3.33)$$

$$\widehat{\theta}(\eta; q) = \theta_0(\eta) + \sum_{m=1}^{\infty} \theta_m(\eta) q^m, \quad (3.34)$$

where

$$f_m(\eta) = \frac{1}{m!} \left. \frac{\partial^m \widehat{f}(\eta; q)}{\partial q^m} \right|_{q=0}, \quad \theta_m(\eta) = \frac{1}{m!} \left. \frac{\partial^m \widehat{\theta}(\eta; q)}{\partial q^m} \right|_{q=0}. \quad (3.35)$$

Note that the zeroth-order deformation Eqs. (3.25) and (3.26) contain two auxiliary parameters \hbar_f and \hbar_θ . The convergence of the series (3.25) and (3.26) depend on these parameters. Assuming that \hbar_f and \hbar_θ are selected such that the above series are convergent at $q = 1$, then using Eqs. (3.31) and (3.32), the series solutions are

$$f(\eta) = f_0(\eta) + \sum_{m=1}^{\infty} f_m(\eta), \quad (3.36)$$

$$\theta(\eta) = \theta_0(\eta) + \sum_{m=1}^{\infty} \theta_m(\eta). \quad (3.37)$$

Differentiate the zeroth-order deformation equations (3.25) and (3.26), m times with respect to q , then setting $q = 0$, and finally dividing them by $m!$, we obtain the m th-order deformations equations as

$$\mathcal{L}_f [f_m(\eta) - \chi_m f_{m-1}(\eta)] = \hbar_f \mathcal{R}_m^f(\eta), \quad (3.38)$$

$$\mathcal{L}_\theta [\theta_m(\eta) - \chi_m \theta_{m-1}(\eta)] = \hbar_\theta \mathcal{R}_m^\theta(\eta). \quad (3.39)$$

$$f_m(0) = 0, \quad f'_m(0) = \beta f''_m(0), \quad f_m(\infty) = 0. \quad (3.40)$$

$$\theta_m(0) = \gamma \theta'_m(0), \quad \theta_m(\infty) = 0. \quad (3.41)$$

where

$$\begin{aligned} \mathcal{R}_m^f(\eta) = & f'''_{m-1} - A \left(f'_{m-1} + \frac{1}{2} \eta f''_{m-1} \right) - A f^2_{m-1} - \lambda f'_{m-1} \\ & + \sum_{k=0}^{m-1} [f_{m-1-k} f''_k - f'_{m-1-k} f'_k] + (1 - \chi_m)(A f^2 \epsilon + \lambda \epsilon + A \epsilon + \epsilon^2), \end{aligned} \quad (3.42)$$

$$\mathcal{R}_m^\theta(\eta) = \text{Pr}^{-1} \theta''_{m-1} - \frac{3}{2} A \theta_{m-1} - A \frac{\eta}{2} \theta'_{m-1} + \sum_{k=0}^{m-1} [f_{m-1-k} \theta'_k - 2 f'_{m-1-k} \theta_k], \quad (3.43)$$

774-8653

$$X_m = \begin{cases} 0, & m \leq 1. \\ 1, & m > 1. \end{cases} \quad (3.44)$$

If we suppose $f_m^*(\eta)$ and $\theta_m^*(\eta)$ as the special solutions of Eqs. (3.38) and (3.39) then from Eqs. (3.38) and (3.39), the general solutions are given by

$$f_m(\eta) = f_m^*(\eta) + C_1 + C_2 \exp(\eta) + C_3 \exp(-\eta), \quad (3.45)$$

$$\theta_m(\eta) = \theta_m^*(\eta) + C_4 \exp(\eta) + C_5 \exp(-\eta), \quad (3.46)$$

where the integral constants C_i , ($i = 1 - 5$) are determined from the boundary conditions (3.40) and (3.41) as

$$C_2 = C_4 = 0, \quad C_3 = \frac{\left. \frac{\partial f_m^*(\eta)}{\partial \eta} \right|_{\eta=0} - \beta \left. \frac{\partial f_m^{*2}(\eta)}{\partial \eta^2} \right|_{\eta=0}}{1 + \beta}, \quad (3.47)$$

$$C_1 = -C_3 - f_m^*(0), \quad C_5 = -\frac{\left. \theta_m^*(\eta) \right|_{\eta=0} - \gamma \left. \frac{\partial \theta_m^*(\eta)}{\partial \eta} \right|_{\eta=0}}{1 + \gamma}.$$

In this way, it is easy to solve the linear non-homogeneous Eqs. (3.38) and (3.39) by using Mathematica one after the other in the order $m = 1, 2, 3, \dots$.

3.3.3 Convergence of the HAM solution

As proved by Liao [12] that, as long as a solution series given by the homotopy analysis method converge, it must be one of the solutions. Therefore, it is important to ensure that the solutions series are convergent. The series solutions (3.36) and (3.37) contain the non-zero auxiliary parameters \hbar_f and \hbar_θ , which can be chosen properly by plotting the so-called \hbar -curves to ensure the convergence of the solutions series and rate of approximation of the HAM solution. To see the range for admissible values of \hbar_f and \hbar_θ , \hbar -curves of $f''(0)$ and $\theta'(0)$ are shown in Fig. 3.1, for 20th-order of approximation when $A = 0.2 = \lambda = \epsilon$, $M = 0.5 = \text{Pr}$ and $\gamma = \beta = 0.2$. From this Fig. it can be seen that \hbar -curves have a parallel lines segment that correspond to the regions $-1.1 \leq \hbar_f \leq -0.2$ and $-1.15 \leq \hbar_\theta \leq -0.2$, respectively. Table 1 is made to show the convergence and comparison of HAM solution for various order of approximations with numerical results when $A = 0.2 = \lambda = \epsilon$, $M = 0.5 = \text{Pr}$ and $\beta = \gamma = 0.2$.

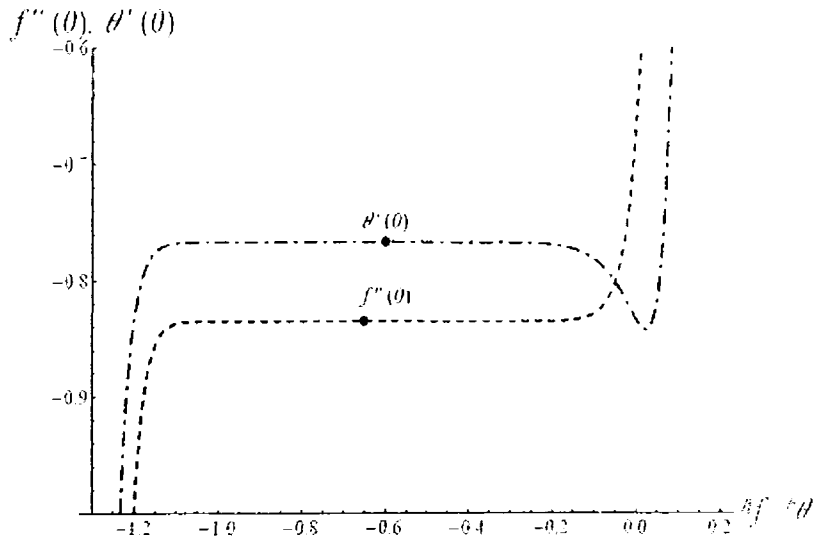


Fig. 3.1: The h-curves of $f''(0)$ and $\theta'(0)$ at the 20th order of approximation: filled circles are the numerical values with $M = 0.5 = Pr$ and $A = \lambda = \epsilon = \gamma = \beta = 0.2$.

Table 3.1: Convergence and comparison of HAM solution for different order of approximation with numerical results when $M = 0.5 = Pr$ and $A = \lambda = \epsilon = \gamma = \beta = 0.2$.

Order of approximations	$-f''(0)$	$-\theta'(0)$
1	0.815741	0.816454
5	0.834424	0.769523
9	0.834491	0.766372
15	0.834491	0.766005
20	0.834491	0.765987
23	0.834491	0.765985
25	0.834491	0.765985
30	0.834491	0.765985
Numerical results	0.834519	0.765986

3.4 Results and discussion

The system of equations (3.9) and (3.10) with boundary conditions (3.11) and (3.12) has been solved both analytically using homotopy analysis method (HAM) and numerically using shooting method [26] with Runge-Kutta algorithm. Figs. (3.2)–(3.11) are plotted in order to analyze the influences of the various involving physical parameters, for example, an unsteadiness parameter A , the magnetic parameter M , the porosity parameter λ , the velocity slip parameter β , the ratio of external flow rate to the stretching rate ϵ , the Prandtl number Pr and the thermal slip parameter γ on the velocity $f'(\eta)$ and temperature $\theta(\eta)$ distributions. The numerical values of the skin-friction coefficient $-f''(0)$ and the rate of heat transfer at the wall (the local Nusselt number) $-\theta'(0)$ for various values of parameters are given in Tables (3.2) – (3.4).

Table 3.2: Numerical values of skin friction coefficient $-f''(0)$ and the local Nusselt number $-\theta'(0)$ for several values of A , M and λ with $\gamma = \beta = 0.2$ and $Pr = \epsilon = 0.5$.

			$-f''(0)$		$-\theta'(0)$	
A	M	λ	HAM	Numerical	HAM	Numerical
0.2	0.5	0.5	0.60449	0.60449	0.83901	0.83901
0.8			0.64108	0.64109	0.95431	0.95425
1.2			0.66376	0.66376	1.0201	1.0201
2.0			0.70545	0.70545	1.1330	1.1330
0.8	0		0.62073	0.62075	0.95657	0.95651
	0.5		0.64108	0.64109	0.95431	0.95425
	1.0		0.69538	0.69548	0.94847	0.94841
	1.5		0.76970	0.76970	0.94099	0.94099
	2.0		0.85193	0.85193	0.93334	0.93334
	0.5	0	0.59900	0.59904	0.95904	0.95900
		0.5	0.64108	0.64109	0.95430	0.95425
		1.0	0.67827	0.67829	0.95028	0.95021
		1.5	0.71165	0.71165	0.94679	0.94679
		2.0	0.74194	0.74195	0.94372	0.94370

Table 3.3: Numerical values of skin friction coefficient $-f''(0)$ and the local Nusselt number $-\theta'(0)$ for several values of ϵ and β with $M = 0.2 = \lambda$.

ϵ	β	$A = 0.8$				$A = 1.2$				$A = 2.0$			
		HAM		Numerical		HAM		Numerical		HAM		Numerical	
		$-f''(0)$	$-\theta'(0)$	$-f''(0)$	$-\theta'(0)$	$-f''(0)$	$-\theta'(0)$	$-f''(0)$	$-\theta'(0)$	$-f''(0)$	$-\theta'(0)$	$-f''(0)$	$-\theta'(0)$
0	0.2	1.0176	0.8710	1.0176	0.8716	1.0865	0.9470	1.0865	0.9473	1.2059	1.0724	1.2059	1.0726
0.5		0.5980	0.9591	0.5981	0.9590	0.6238	1.0240	0.6238	1.0240	0.6707	1.1357	0.6709	1.1357
1.0		0	1.0476	0	1.0472	0	1.1029	0	1.1025	0	1.2013	0	1.2019
1.5		0.7305	1.1300	0.7305	1.1304	0.7479	1.1781	0.7479	1.1780	0.7804	1.2653	0.7805	1.2667
2.0		1.5652	1.2057	1.5652	1.2056	1.5953	1.2483	1.5953	1.2480	1.6515	1.3264	1.6523	1.3269
0.5	0	0.8050	0.9831	0.8051	0.9831	0.8498	1.0467	0.8498	1.0461	0.9345	1.1562	0.9347	1.1561
	0.5	0.4351	0.9386	0.4351	0.9386	0.4491	1.0052	0.4491	1.0050	0.4744	1.1195	0.4745	1.1190
	1	0.3010	0.9206	0.3010	0.9201	0.3081	0.9889	0.3080	0.9889	0.3203	1.1060	0.3203	1.1068
	1.5	0.2307	0.9106	0.2307	0.9106	0.2349	0.9801	0.2347	0.9801	0.2421	1.0989	0.2422	1.0987
	2.0	0.1871	0.9043	0.1872	0.9041	0.1900	0.9746	0.1900	0.9746	0.1947	1.0946	0.1948	1.0949

Table 3.4: Numerical values of the local Nusselt number $-\theta'(0)$ for several values of A , Pr and γ with $M = \lambda = \beta = 0.2$ and $\epsilon = 0.5$.

Pr	γ	$A = 0.8$		$A = 1.2$	
		$-\theta'(0)$		$-\theta'(0)$	
		HAM	Numerical	HAM	Numerical
0.1	0.2	0.46416	0.46410	0.50277	0.50271
0.3		0.76908	0.76901	0.82519	0.82511
0.7		1.1024	1.1021	1.1729	1.1724
1.0		1.2700	1.2700	1.3462	1.3453
1.5		1.4791	1.4761	1.5610	1.5604
2.0		1.6384	1.6315	1.7239	1.7211
3.0		1.8761	1.8701	1.9653	1.9647
5.0		2.1916	2.1901	2.2834	2.2801
0.7	0	1.4143	1.4149	1.5324	1.5329
	0.5	0.82844	0.82854	0.86763	0.86796
	1.0	0.58579	0.58586	0.60512	0.60526
	1.5	0.45309	0.45317	0.46456	0.46461
	2.0	0.36940	0.36983	0.37699	0.37699
	3.0	0.26975	0.26979	0.27378	0.27384
	5.0	0.17522	0.17584	0.17691	0.17613
	10.0	0.09339	0.09339	0.09387	0.09387

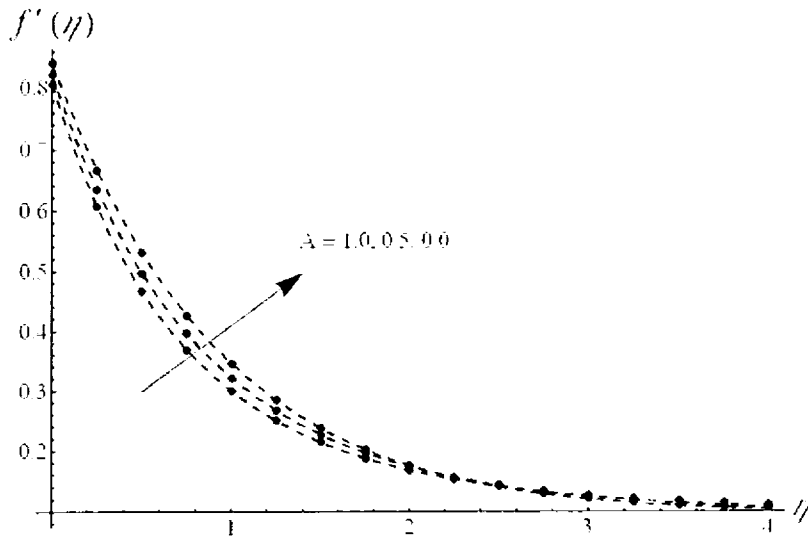


Fig. 3.2: The velocity profile $f'(\eta)$ versus η for various values of unsteadiness parameter A : dashed lines are numerical solution and filled circle are HAM solution at 12-th order of approx. with $M = 0.2 = \beta$ and $\lambda = 0.1 = \epsilon$.

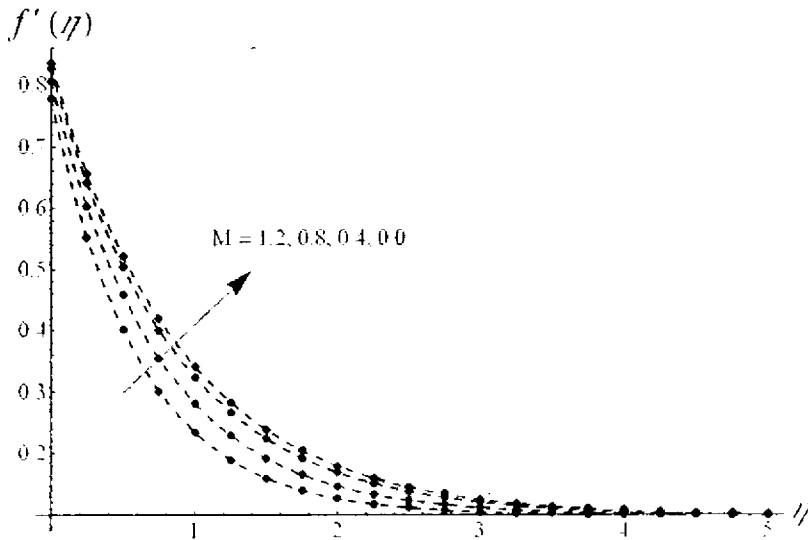


Fig. 3.3: The velocity profile $f'(\eta)$ versus η for various values of magnetic parameter M : dashed lines are numerical solution and filled circle are HAM solution at 12-th order of approx. with $A = 0.2 = \beta$ and $\lambda = 0.1 = \epsilon$.

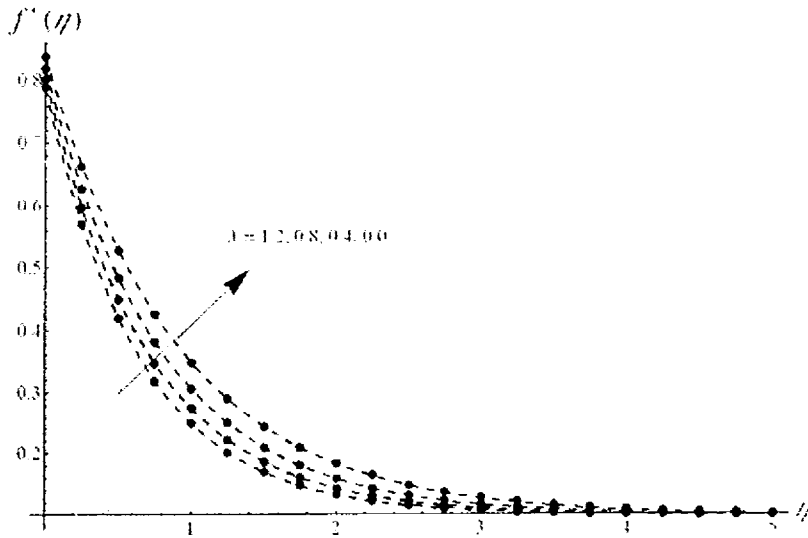


Fig. 3.4: The velocity profile $f'(\eta)$ versus η for various values of porous medium λ : dashed lines are numerical solution and filled circle are HAM solution at 12-th order of approx. with $A = M = \beta = 0.2$ and $\epsilon = 0.1$.

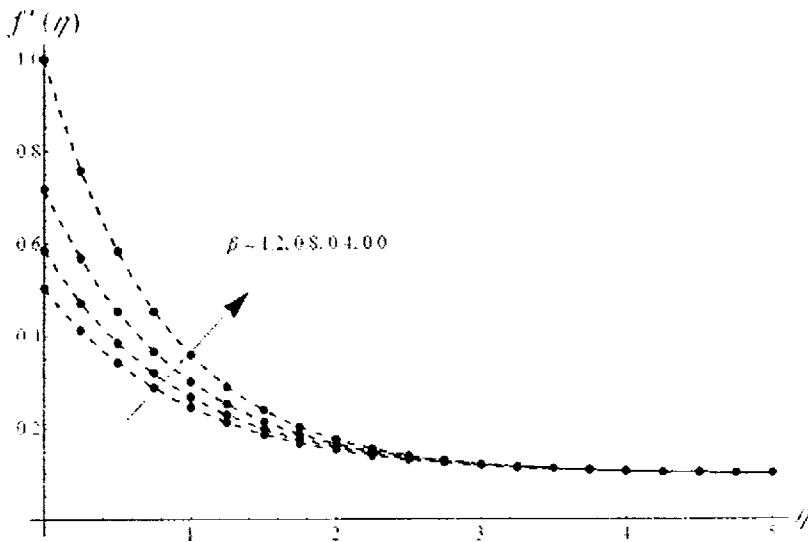


Fig. 3.5: The velocity profile $f'(\eta)$ versus η for various values of slip parameter β : dashed lines are numerical solution and filled circle are HAM solution at 12-th order of approx. with $A = M = \lambda = 0.2$ and $\epsilon = 0.1$.

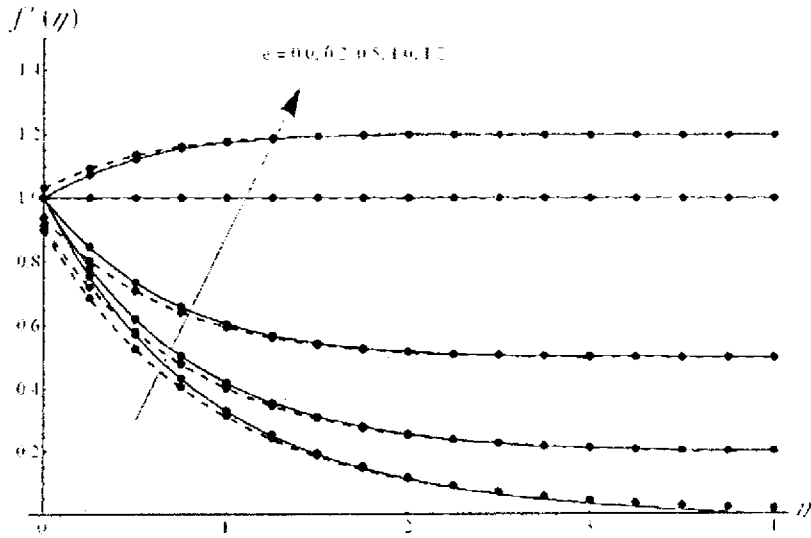


Fig. 3.6: The velocity profile $f'(\eta)$ versus η for various values of stagnation point parameter ϵ : solid / dashed lines are numerical solution and filled circle are HAM solution at 12-th order of approx. with $A = M = 0.2$ and $\lambda = 0.1$.

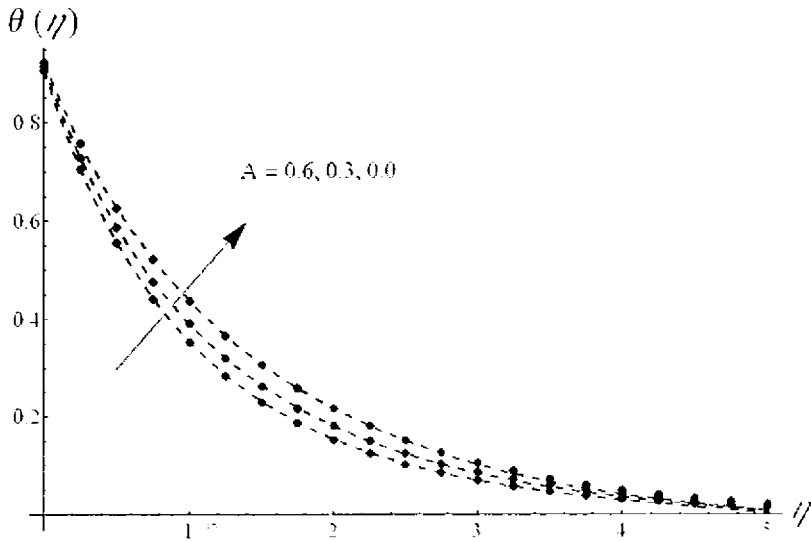


Fig. 3.7: The temperature profile $\theta(\eta)$ versus η for various values of unsteadiness parameter A : dashed lines are numerical solution and filled circle are HAM solution at 12-th order of approx. with $M = \beta = 0.2$, $\lambda = \epsilon = \gamma = 0.1$ and $Pr = 0.5$.

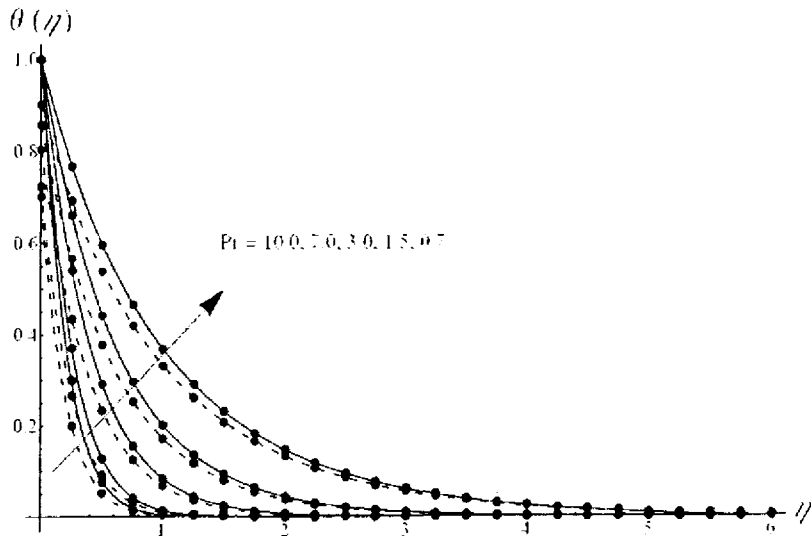


Fig. 3.8: The temperature profile $\theta(\eta)$ versus η for various values of Prandtl number Pr : solid / dashed lines are numerical solution and filled circle are HAM solution at 12-th order of approx. with $A = M = \beta = 0.2$ and $\lambda = \epsilon = 0.1$.

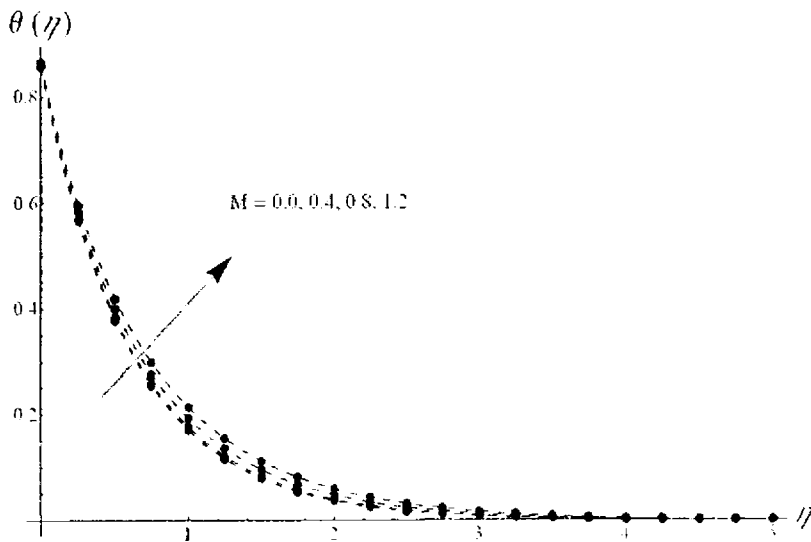


Fig. 3.9: The temperature profile $\theta(\eta)$ versus η for various values of magnetic parameter M : dashed lines are numerical solution and filled circle are HAM solution at 12-th order of approx. with $A = \beta = 0.2$, $\epsilon = \lambda = \gamma = 0.1$ and $Pr = 1.5$.

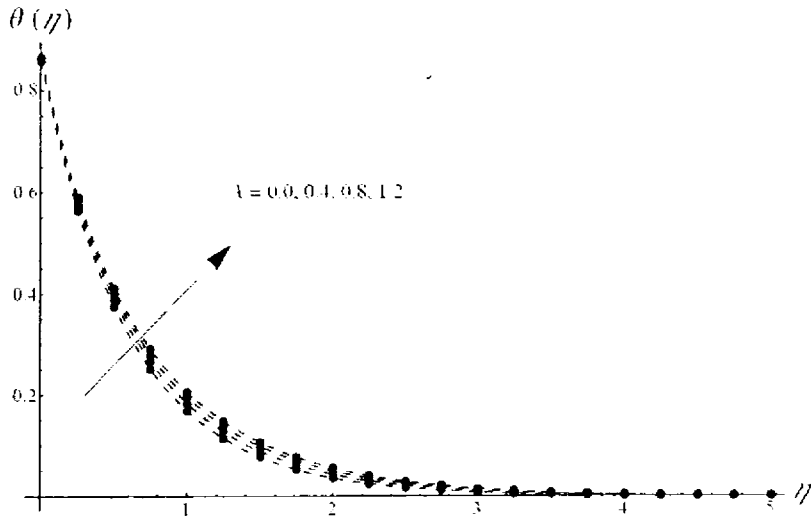


Fig. 3.10: The temperature profile $\theta(\eta)$ versus η for various values of porous medium λ : dashed lines are numerical solution and filled circle are HAM solution at 12-th order of approx. with $A = M = \beta = 0.2$, $Pr = 1.5$ and $\epsilon = \gamma = 0.1$.

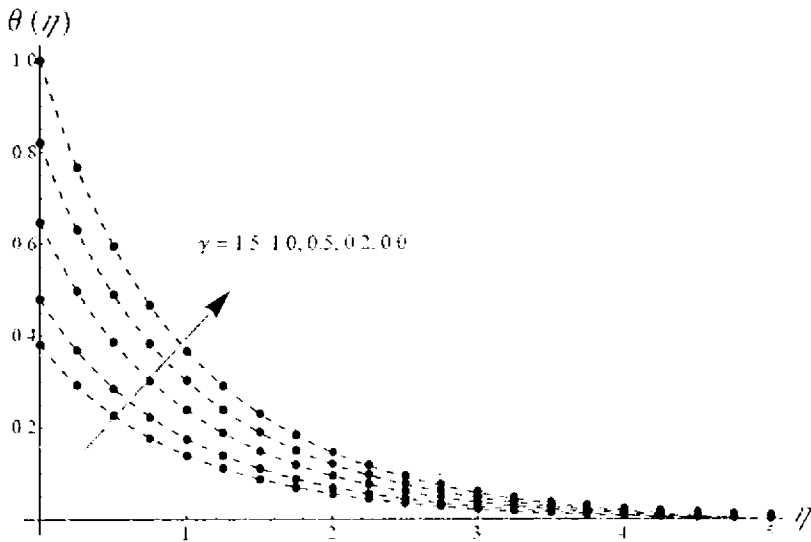


Fig. 3.11: The temperature profile $\theta(\eta)$ versus η for various values of slip parameter γ : dashed lines are numerical solution and filled circle are HAM solution at 12-th order of approx. with $A = M = \beta = 0.2$, $\lambda = \epsilon = 0.1$ and $Pr = 0.7$.

Table 3.2 shows the analytical and numerical values of the skin-friction coefficient $-f''(0)$ and the local Nusselt number $-\theta'(0)$ for various values of A , M , and λ when $\gamma = \beta = 0.2$ and $Pr = \epsilon = 0.5$. It is noted that the magnitudes of $-f''(0)$ and $-\theta'(0)$ increase for large values of A . We can also be see from this Table that the magnitudes of the shear stress at the wall $-f''(0)$ increase by increasing the values of M and λ but the rate of heat transfer at the wall decrease by increasing the values of M and λ . The numerical values of $-f''(0)$ and $-\theta'(0)$ for several values of ϵ , β and A is given in Table 3.3. It is found that for fixed values of ϵ and β , the magnitude of $-f''(0)$ and $-\theta'(0)$ increase by increasing A . It is further seen that the magnitude of the skin-friction coefficient $-f''(0)$ decreases for $\epsilon < 1$ and increases for $\epsilon > 1$ for fixed values of A and β . On the other hand, the magnitude of $-f''(0)$ decreases as the slip parameter β increases. However, the rate of heat transfer at the wall $-\theta'(0)$ increases for large values of ϵ , where as it decreases by increasing the values of β . Table 3.4 is prepared to show the numerical values of the local Nusselt number $-\theta'(0)$ for different values of Pr , γ and A when $A = M = \beta = 0.2$ and $\epsilon = 0.1$. It is observed that for fixed values of A , the magnitude of the local Nusselt number increases (decreases) for large values of Pr (γ). It is also worth-mentioning observation from the Tables that both solutions are in good agreement.

Fig. 3.2 shows the effects of an unsteadiness parameter A on the velocity component $f'(\eta)$ when $M = 0.2 = \beta$ and $\lambda = 0.1 = \epsilon$. Both the velocity and the boundary layer thickness are decreased as an unsteadiness parameter A increases. Fig. 3.3 elucidates the influence of the magnetic parameter M on the velocity $f'(\eta)$ when $A = 0.2 = \beta$ and $\lambda = 0.1 = \epsilon$. It is noted from this Fig. that the velocity decreases by increasing the values of magnetic parameter M . This is because for the present problem the magnetic force acts as a resistance to the flow. The boundary layer thickness is also decreased as M increases. The change in the velocity field $f'(\eta)$ for different values of porosity parameter λ can be seen in Fig. 3.4. It is found that the velocity $f'(\eta)$ is a decreasing function of λ . The boundary layer thickness is decreased for large values of λ . Fig. 3.5 depicts the variations of the velocity slip parameter β on the velocity component $f'(\eta)$ when $\epsilon = 0.1$. It is observed that the velocity is decreased by increasing the values of the velocity slip parameter β . It is also noted that for $\beta = 0$ (no-slip condition), the values of f' is equal to 1, which shows the standard condition for stretching flow at $\eta = 0$. Fig. 3.6 shows the effects of the ratio of the external flow rate to the stretching rate ϵ on the velocity field

$f'(\eta)$: solid lines (for no-slip condition $\beta = 0$) and dashed lines (for slip condition $\beta = 0.2$), respectively. It is found that the velocity $f'(\eta)$ is increased for large values of ϵ for both $\beta = 0$, $\beta = 0.2$ but this change in the velocity in case of velocity slip parameter ($\beta = 0.2$) is smaller for $\epsilon < 1$ and larger for $\epsilon > 1$ near the wall when compared with the case of no-slip condition ($\beta = 0$).

Fig. 3.7 gives the influences of an unsteadiness parameter A on the temperature distribution $\theta(\eta)$ when thermal slip parameter $\gamma = 0.1$. Both the temperature profile and the thermal boundary layer thickness are decreased as A increases. Fig. 3.8 shows the change in the temperature $\theta(\eta)$ for the several values of Prandtl number Pr : solid lines (for no-thermal slip $\gamma = 0$) and dashed lines (for thermal slip $\gamma = 0.1$). It can be seen from this Fig. that the temperature decreases by increasing the values of Pr . The thermal boundary layer thickness also decreases for large values of Prandtl number. Fig. 3.9 gives the variations in the temperature distribution $\theta(\eta)$ for various values of a magnetic parameter M . One can see that the temperature is an increasing function of a magnetic parameter M , and the thermal boundary layer thickness also increases as M is increased. Fig. 3.10 presents the effects of a porosity parameter λ on the temperature distribution θ . It is found from this Fig. that both the temperature and the thermal boundary layer thickness are increasing function of λ . It is also noticed from these Figs. (3.9 and 3.10) that for large values of M and λ , the change in temperature is small, this is because both parameters have no influence in the energy equation directly. The temperature field $\theta(\eta)$ for several values of thermal slip parameter γ is shown in Fig. 3.11. It is observed that as the thermal slip parameter increases, less heat is transformed from the sheet to the fluid, therefore the temperature $\theta(\eta)$ decreases by increasing the values of the thermal slip parameter γ .

Bibliography

- [1] B. C. Sakiadis, Boundary layer behavior on continuous solid surfaces: I. Boundary-layer equations for two-dimensional and axisymmetric flow, *AIChE. J.* **7**(1) (1961) 26 – 28.
- [2] B. C. Sakiadis, Boundary layer behaviour on continuous solid surface: II. Boundary layer behavior on continuous flat surface, *AIChE. J.* **7**(1) (1961) 221 - 225.
- [3] L. J. Crane, Flow past a stretching plane, *Z Angew Math Phys.* **21** (1970) 645 – 647.
- [4] C. Y. Wang, Liquid film on unsteady stretching sheet, *Quart. J. Appl. Math.* **48** (1990) 601.
- [5] H. T. Andersson, J. B. Aarseth, B. S. Dandapat, Heat transfer in a liquid film on an unsteady stretching surface, *Int J Heat Transfer.* **43**(2000) 69 – 74.
- [6] E. M. A. Elbashaeshy and M. A. A. Bazid, Heat transfer over an unsteady stretching surface, *Heat Mass Transfer.* **41** (2004) 1 – 4.
- [7] R. Tsai, K.H. Huang, J.S. Huang, Flow and heat transfer over an unsteady stretching surface with non-uniform heat source, *Int. Com. Heat Mass Transfer.* **35** (2008) 1340–1343.
- [8] A. Ishak, R. Nazar, I. Pop Heat transfer over an unsteady stretching permeable surface with prescribed wall temperature, *Nonlinear Anal: Real World Appl.* **10** (2009) 2909 – 2913.
- [9] S. Mukhopadhyay, Effect of thermal radiation on unsteady mixed convection flow and heat transfer over a porous stretching surface in medium, *Int J. Heat Mass Transfer.* **52** (2009) 3261 – 3265.

- [10] Mohamed Abd El-Aziz. Radiation effect on the flow and heat transfer over an unsteady stretching sheet, *Int. Com. Heat Mass Transfer*. **36** (2009) 521 – 524.
- [11] S. Mukhopadhyay. Unsteady boundary layer flow and heat transfer past a porous stretching sheet in presence of variable and thermal diffusivity, *Int. J. Heat Mass Transfer*. **52** (2009) 5213 – 5217.
- [12] S. J. Liao, *Beyond Perturbation, Introduction To Homotopy Analysis Method*, Boca Raton: Chapman & Hall/CRC Press; 2003.
- [13] S. J. Liao, A uniformly valid analytical solution of 2D viscous flow past a semi-infinite flat plate, *J. Fluid Mech.* **385** (1999) 101.
- [14] S. J. Liao, A new branch of boundary-layer flow over an impermeable stretched plate, *Int. J. Non-Linear Mech.* **42** (2007) 819.
- [15] H. Xu, S. J. Liao, and G.X. Wu, A family of new solutions on the wall jet, *European J. Mech. B/Fluid*. **27** (2008) 322.
- [16] S. Abbasbandy and F. S. Zakaria, Soliton solutions for the fifth-order KdV equation with the homotopy analysis method, *Nonlinear Dyn.* **51** (2008) 83.
- [17] S. Abbasbandy and E. J. Parkes, Solitary smooth solutions for the Camassa-Holm equation by means of homotopy analysis method, *Chaos, Solitons & Fractals*. **36** (2008) 581.
- [18] S. Abbasbandy, Homotopy analysis method for radiation equations, *Int. Com. Heat Mass Transfer*. **34** (2007) 380.
- [19] T. Hayat, Z. Abbas and M. Sajid, Heat and mass transfer analysis on the flow of a second grade fluid in the presence of chemical reaction, *Phys. Lett. A*. **372** (2008) 2400
- [20] T. Hayat, M. Sajid, and M. Ayub, A note on series solution for generalized Couette flow, *Comm. Non-linear Sci. Numer. Simu.* **12** (2007) 1481.
- [21] Z. Abbas, M. Sajid, and T. Hayat, MHD boundary layer flow of an upper-convected Maxwell fluid in porous channel, *Theor. Comp. Fluid Dyn.* **20** (2006) 229.

- [22] T. Hayat, Z. Abbas and M. Sajid, Series solution for the upper-convected Maxwell fluid over a porous plate. *Lett. A.* **358** (2006) 396.
- [23] T. Hayat, M.A. Farooq, T. Javed and M. Sajid, Partial slip effect on the flow and heat transfer characteristics in a third grade fluid, *Nonlinear Analysis: Real World Applications* (In Press).
- [24] T. Hayat and T. Javed, On analytic solution for generalized three-dimensional MHD flow³ over a porous stretching sheet, *Phy. Lett. A.* **370** (2007) 243.
- [25] M. Sajid, T. Hayat and S. Asghar, Non-similar analytic solution for MHD flow and heat transfer in a third-order fluid over a stretching sheet, *Int. J. Heat Mass Transfer.* **50** (2007) 1723.
- [26] T. Y. Na, *Computational Methods In Engineering Boundary Value Problems*, New York, (1979).